Inorg. Chem. **2008**, *47*, 8286−8293

Topology Analysis and Nonlinear-Optical-Active Properties of Luminescent Metal−Organic Framework Materials Based on Zinc/Lead Isophthalates

Lei Zhang,[†,‡] Ye-Yan Qin,[†] Zhao-Ji Li,[†] Qi-Pu Lin,[†,‡] Jian-Kai Cheng,[†] Jian Zhang,[†] and Yuan-Gen Yao*[,†]

The State Key Laboratory of Structural Chemistry, Fujian Institute of Research on the Structure of Matter, The Chinese Academy of Sciences, Fuzhou, Fujian 350002, P. R. China, and Graduate School of the Chinese Academy of Sciences, Bejing 100039, P. R. China

Received May 15, 2008

Two 3D Zn(II) and Pb(II) isophthalates, $[Zn(ip)]_n$ (**1**) and $[Pb_4(\mu_4\text{-}O)(ip)_3(H_2O)]_n$ (**2**) (H_2ip = isophthalic acid), have been prepared under hydro(solvo)thermal conditions and characterized by single-crystal X-ray diffraction. The two complexes crystallize in different space groups ($P4_32_12$ for **1** and $P2_1/c$ for **2**) and have different bridging modes of the ip ligand. The 3D framework of **1** is constructed by the interconnection of ZnO_4 polyhedra via ip ligands, which represents a chiral net with PtS-type topology. In contrast, complex **2** is formed by the combination of Pb_4O-cluster secondary building units and has a novel $(3.4.5)(3^2.4^5.5^6.6^7.7^2)$ topology, which is the first ever example of a (3,7)-connected net. Complex **1** displays a second harmonic generation efficiency of about 1.5 times that of KH_2PO_4. Optical properties and thermal stabilities of the two complexes have been studied. Additionally, the calculations of band structure and density of states of **1** have also been performed with the density functional theory method.

Introduction

Much attention is currently devoted to the research of novel materials based on metal−organic frameworks (MOFs), mostly motivated by their intriguing structures, new topologies, and potential applications.[1] Of particular interest is the creation of homochiral MOF materials, which may have advanced applications in asymmetric catalysis and enantioselective separation.[2] Among them, new second-order nonlinear optical (NLO) materials are of great importance due to their future applications in photonic technologies.[3] Compared to widely used inorganic NLO crystals based on borates and phosphates, they offer a large variety of molecular structures and a great diversity of tunable electronic properties by virtue of the metal center.[4] Up to now, Dr. Lin and other researchers have reported lots of such materials, mostly based on unsymmetrical pyridinecarboxylates and aromatic carboxylate ligands.[5] However, isophthalic

* Author to whom correspondence should be addressed. Phone: +86-591-83711523. Fax: +86-591-83714946. E-mail: yyg@fjirsm.ac.cn.
† Fujian Institute of Research on the Structure of Matter.
‡ Graduate School of the Chinese Academy of Sciences.

(1) (a) Ockwig, N. W.; Delgado-Friedrichs, O.; O'Keefee, M.; Yaghi, O. M. *Acc. Chem. Res.* **2005**, *38*, 176. (b) Hill, R. J.; Long, D. L.; Champness, N. R.; Hubberstey, P.; Schroöder, M. *Acc. Chem. Res.* **2005**, *38*, 377. (c) Yaghi, O. M.; Li, H.; Davis, C.; Richardson, D.; Groy, T. L. *Acc. Chem. Res.* **1998**, *31*, 474. (d) Leininger, S.; Olenyuk, B.; Stang, P. J. *Chem. Rev.* **2000**, *100*, 853. (e) Sato, O.; Iyoda, T.; Fujishima, A.; Hashimoto, K. *Science* **1996**, *271*, 49. (f) Kitagawa, S.; Kitaura, R.; Noro, S. *Angew. Chem., Int. Ed.* **2004**, *43*, 2334. (g) Belof, J. L.; Stern, A. C.; Eddaoudi, M.; Space, B. *J. Am. Chem. Soc.* **2007**, *129*, 15202. (h) Eddaoudi, M.; Moler, D. B.; Li, H. L.; Chen, B. L.; Reineke, T. M.; O'Keeffe, M.; Yaghi, O. M. *Acc. Chem. Res.* **2001**, *34*, 319. (i) Livage, C.; Guillou, N.; Marrot, J.; Férey, G. *Chem. Mater.* **2001**, *13*, 4387.

(2) (a) Zhang, J.; Bu, X. H. *Angew. Chem., Int. Ed.* **2007**, *46*, 6115. (b) Zhang, J.; Liu, R.; Feng, P. Y.; Bu, X. H. *Angew. Chem., Int. Ed.* **2007**, *46*, 8388. (c) Zhang, J.; Chen, S. M.; Valle, H.; Wong, M.; Austria, C.; Cruz, M.; Bu, X. H. *J. Am. Chem. Soc.* **2007**, *129*, 14168. (d) Seo, J. S.; Whang, D.; Lee, H.; Jun, S. I.; Oh, J.; Jeon, Y. J.; Kim, K. *Nature* **2000**, *404*, 982. (e) Zeng, M. H.; Wang, B.; Wang, X. Y.; Zhang, W. X.; Chen, X. M.; Gao, S. *Inorg. Chem.* **2006**, *45*, 7069. (f) Guillou, N.; Livage, C.; Drillon, M.; Férey, G. *Angew. Chem., Int. Ed.* **2003**, *42*, 5314.

(3) (a) Zhao, H.; Qu, Z. R.; Ye, H. Y.; Xiong, R. G. *Chem. Soc. Rev.* **2008**, *37*, 84. (b) Ye, Q.; Li, Y. H.; Song, Y. M.; Huang, X. F.; Xiong, R. G.; Xue, Z. L. *Inorg. Chem.* **2005**, *44*, 3618. (c) Ye, Q.; Tang, Y. Z.; Wang, X. S.; Xiong, R. G. *Dalton Trans.* **2005**, 1570. (d) Ye, Q.; Li, Y. H.; Wu, Q.; Song, Y. M.; Wang, J. X.; Zhao, H.; Xiong, R. G.; Xue, Z. L. *Chem.−Eur. J.* **2005**, *11*, 988. (e) Maggard, P. A.; Stern, C. L.; Poeppelmeier, K. R. *J. Am. Chem. Soc.* **2001**, *123*, 7742. (f) Abrahams, B. F.; Jackson, P. A.; Roboson, R. *Angew. Chem., Int. Ed.* **1998**, *37*, 2656.

10.1021/ic800871r CCC: $40.75
Published on Web 08/16/2008

Table 1. Crystal Data and Structure Refinements for Compounds **1** and **2**

param	**1**	**2**
formula	$C_{16}H_8Zn_2O_8$	$C_{24}H_{14}Pb_4O_{14}$
fw	459.00	1355.11
temp (K)	293(2)	293(2)
cryst syst	tetragonal	monoclinic
space group	$P4_32_12$	$P2_1/c$
a (Å)	9.6432(4)	15.299(3)
b (Å)	9.6432(4)	13.601(2)
c (Å)	32.2446(18)	14.040(3)
β (deg)	90	112.600(2)
v (Å^3)	2998.5(2)	2697.2(9)
Z	8	4
flack parameter	0.01(1)	
D_{calcd} (g cm^{-3})	2.033	3.337
μ (mm^{-1})	3.247	24.965
GOF	1.082	1.043
R1[a] ($I > 2\sigma(I)$)	0.0624	0.0275
wR2[a] (all data)	0.1697	0.0625

[a] $R1 = \sum||F_o| - |F_c||/\sum|F_o|$; $wR2 = \{\sum[w(F_o^2 - F_c^2)^2]/\sum[w(F_o^2)^2]\}^{1/2}$; $w = 1/[\sigma^2(F_o^2) + (aP)^2 + bP]$, where $P = [\max(F_o^2,0) + 2F_c^2]/3$ for all data.

acid, which is an extremely familiar ligand, has rarely been reported in this area.[6] And despite tremendous progress in these areas, fabrication of NLO MOF materials with high thermal stabilities remains a challenge.

Network topology has been proved to be an important and essential aspect of the design and analysis of MOF materials.[1a,b,7] A growing number of structural types have been reported, most of which are based on three-, four-, or six-connected topologies.[8] However, MOFs formed with connectivity greater than six are still rare because the construction of such systems is severely hampered by the available number of coordination sites at the metal centers. In fact, there are only three reported examples of uninodal seven-connected nets and no examples of nets with mixed connectivity containing seven-connected nodes.[9] In order to obtain highly connected MOFs, the attempt to replace metal ions with metal clusters as nodes has been an effective route, due to the enhancement of coordination numbers and reduction of steric hindrances.[10]

In this context, we have employed isophthalic acid ligands with Zn^{II} and Pb^{II} ions and successfully obtained two novel 3D frameworks, $[Zn(ip)]_n$ (**1**) and $[Pb_4(\mu_4\text{-}O)(ip)_3(H_2O)]_n$ (**2**). Complex **1** represents a chiral framework with a PtS-type topology and shows distinct NLO properties. We have also calculated its band structure, which is rarely performed on MOF materials. Complex **2** shows unprecedented (3,7)-connected $(3.4.5)(3^2.4^5.5^6.6^7.7^2)$ topology in which the tetrahedral Pb_4O clusters act as seven-connected nodes and part of the ip groups act as three-connected nodes. Both of the complexes exhibit fluorescence properties and high stabilities.

Experimental Section

General Considerations. Commercially available reagents were used as received without further purification. All syntheses were carried out in 23 mL poly(tetrafluoroethylene)-lined stainless steel containers under autogenous pressure. The elemental analyses were performed on an EA1110 CHNS-0 CE elemental analyzer. The IR spectroscopy was recorded on a PECO (U.S.A.) SpectrumOne spectrophotometer with pressed KBr pellets. The thermal decomposition behavior was analyzed by thermogravimetric analysis−mass spectrometry (TGA-MS) using a NETSCH STA-449C thermoanalyzer coupled with a NETSCH QMS403C massspectrometer. The fluorescence measurements were performed on a Cray Eclipse. The optical diffuse reflectance spectrum was measured at room temperature with a Perkin-Elmer Lambda 900 UV/vis spectrophotometer. A $BaSO_4$ plate was used as a standard (100% reflectance). The phase purity and crystallinity of each product were checked by powder XRD using a Rigaku Dmax2500 diffractometer with Cu Kα radiation (λ = 1.54056 Å). A step size of 0.05° and a counting time of 1.2 s/step were applied in a 2θ range of 5.00−55.00°.

Synthesis of $[Zn(ip)]_n$ (1). A mixture of H_2ip (0.165 g, 1.0 mmol), melamine (0.067 g, 0.5 mmol), NaOH (0.039 g, 1.0 mmol), and $Zn(NO_3)_2\cdot 6H_2O$ (0.605 g, 2.0 mmol) was placed in a 23 mL Teflon liner; 15 mL of water was then added. The resulting mixture was sealed in a Parr autoclave. The autoclave was then placed in a programmable furnace and heated to 160 °C. The temperature was held for 3 days, and then the reactant mixture was cooled at a rate of 0.5 °C min^{-1} to form colorless sheet crystals of **1**. Yield: 80%. Anal. calcd (%) for $C_{16}H_8Zn_2O_8$: C, 41.87; H, 1.76. Found: C, 42.02; H, 1.71%. IR (solid KBr pellet, v/cm^{-1}) for complex **1**: 3394 (w), 1601 (s), 1558 (s), 1538 (s), 1467 (s), 1408 (s), 1087 (w), 932 (w), 851 (w), 751 (m), 732 (m).

Synthesis of $[Pb_4(\mu_4\text{-}O)(ip)_3(H_2O)]_n$ (2). A mixture of H_2ip (0.166 g, 1.0 mmol), melamine (0.063 g, 0.5 mmol), NaOH (0.041 g, 1.0 mmol), and $Pb(OAc)_2\cdot 3H_2O$ (0.770 g, 2.0 mmol) was placed in a 23 mL Teflon liner; 5 mL of ethanol and 10 mL of water were then added. The resulting mixture was sealed in a Parr autoclave.

(4) (a) Cariati, E.; Pizzotti, M.; Roberto, D.; Tessore, F.; Ugo, R. *Coord. Chem. Rev.* **2006**, *250*, 1210. (b) Janiak, C. *Dalton Trans.* **2003**, 2781. (c) Bella, S. D. *Chem. Soc. Rev.* **2001**, *30*, 355. (d) Maury, O.; Bozec, H. L. *Acc. Chem. Res.* **2005**, *38*, 691.

(5) (a) Evans, O. R.; Lin, W. *Acc. Chem. Res* **2002**, *35*, 511, and references therein. (b) Zang, S.; Su, Y.; Li, Y.; Ni, Z.; Meng, Q. *Inorg. Chem.* **2006**, *45*, 174. (c) Wang, L.; Yang, M.; Li, G.; Shi, Z.; Feng, S. *Inorg. Chem.* **2006**, *45*, 2474. (d) Zhou, Y.; Yuan, D.; Wu, B.; Wang, R.; Hong, M. *New J. Chem.* **2004**, *28*, 1590.

(6) (a) Kirillov, A. M.; Karabach, Y. Y.; Haukka, M.; da Silva, M. F. C. G.; Sanchiz, J.; Kopylovich, M. N.; Pombeiro, A. J. L. *Inorg. Chem.* **2008**, *47*, 162. (b) Arbuse, A.; Anda, C.; Martinez, M. A.; Perez-Miron, J.; Jaime, C.; Parella, T.; Llobet, A. *Inorg. Chem.* **2007**, *46*, 10632. (c) Mahata, P.; Ramya, K. V.; Natarajan, S. *Dalton Trans.* **2007**, 4017. (d) Luo, F.; Batten, S. R.; Che, Y. X.; Zheng, J. M. *Chem.—Eur. J.* **2007**, *13*, 4948. (e) Zhang, L.; Li, W.; Zhang, J.; Li, Z. J.; Qin, Y. Y.; Cheng, J. K.; Yao, Y. G. *Inorg. Chem. Commun.* **2008**, *11*, 279.

(7) (a) Wells, A. F. *Three-Dimensional Nets and Polyhedra*; Wiley: New York, 1977. (b) Batten, S. R.; Robson, R. *Angew. Chem., Int. Ed.* **1998**, *37*, 1460. (c) Batten, S. R.; Robson, R. *Angew. Chem., Int. Ed.* **1998**, *110*, 1558. (d) Batten, S. R. *CrystEngComm* **2001**, *3*, 67. (e) Blake, A. J.; Champness, N. R.; Hubberstey, P.; Li, W. S.; Withersby, M. A.; Schröder, M. *Coord. Chem. Rev.* **1999**, *183*, 117. (f) Moulton, B.; Zaworotko, M. J. *Chem. Rev.* **2001**, *101*, 1629. (g) Carlucci, L.; Ciani, G.; Proserpio, D. M. *Coord. Chem. Rev.* **2003**, *246*, 247.

(8) (a) Férey, G.; Mellot-Draznieks, C.; Serre, C.; Millange, F. *Acc. Chem. Res.* **2005**, *38*, 217. (b) Hagrman, P. J.; Hagrman, D.; Zubieta, J. *Angew. Chem., Int. Ed.* **1999**, *38*, 2638. (c) Papaefstathiou, G. S.; MacGillivray, L. R. *Coord. Chem. Rev.* **2003**, *246*, 169. (d) Rao, C. N. R.; Natarajan, S.; Vaidhyanathan, R. *Angew. Chem., Int. Ed.* **2004**, *43*, 1466.

(9) (a) Long, D. L.; Blake, A. J.; Champness, N. R.; Wilson, C.; Schröder, M. *Angew. Chem., Int. Ed.* **2001**, *40*, 2443. (b) Morris, J. J.; Noll, B. C.; Henderson, K. W. *Chem. Commun.* **2007**, 5191.

(10) (a) Zhang, X. M.; Fang, R. Q.; Wu, H. S. *J. Am. Chem. Soc.* **2005**, *127*, 7670. (b) Wang, X. L.; Qin, C.; Wang, E. B.; Su, Z. M.; Xu, L.; Batten, S. R. *Chem. Commun.* **2005**, 4789. (c) Chun, H.; Kim, D.; Dybtsev, D. N.; Kim, K. *Angew. Chem., Int. Ed.* **2004**, *43*, 971. (d) Pan, L.; Liu, H.; Lei, X.; Huang, X.; Olson, D. H.; Turro, N. J.; Li, J. *Angew. Chem., Int. Ed.* **2003**, *42*, 542.

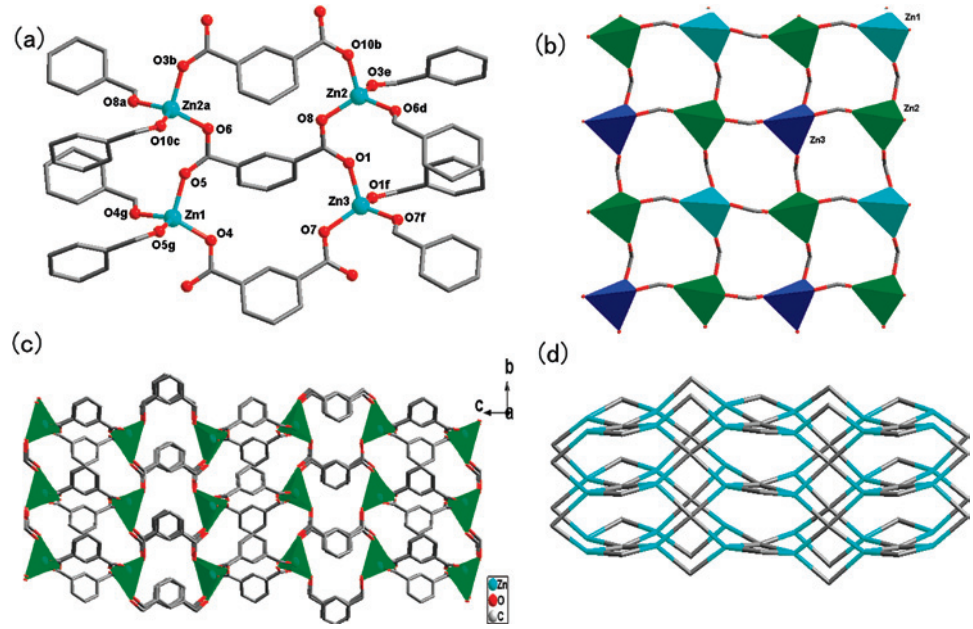

Figure 1. (a) Details of the coordination environments of Zn1, Zn2, and Zn3. (b) Zn−carboxylate layer with $Zn_4(COO)_4$ rings. Color code: Zn1, cambridge blue; Zn2, green; Zn3, navy blue. (c) View of the 3D framework of **1**. (d) A schematic diagram of the PtS topology of **1**.

Table 2. Coordination Modes of the Carboxylate Functions of ip^{2-} in **1** and **2**

Tetradentate	
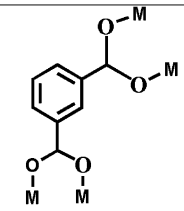 μ_4-O,O′,O″,O‴	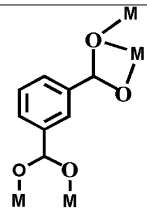 μ_4-(η_2-O,O′),O,O″,O‴
Pentadentate	**Hexadentate**
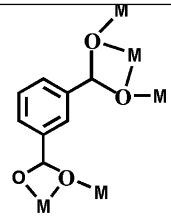 μ_5-(η_2-O,O′),(η_2-O″,O‴),O,O″,O‴	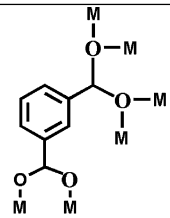 μ_6-O,O,O′,O′,O″,O‴

The autoclave was then placed in a programmable furnace and heated to 160 °C. The temperature was held for 3 days, and then the reactant mixture was cooled at a rate of 0.5 °C min^{-1} to form colorless sheet crystals of **2**. Yield: 60%. Anal. calcd (%) for $C_{24}H_{14}Pb_4O_{14}$: C, 21.27; H, 1.04. Found: C, 21.41; H, 1.01%. IR (solid KBr pellet, v/cm^{-1}) for complex **2**: 3737 (vw), 3012 (w), 2319 (w), 1602 (m), 1518 (s), 1432 (m), 1362 (vs), 1157 (m), 818 (w), 739 (m), 710 (m), 518 (w).

X-Ray Crystallography. Suitable single crystals of **1** and **2** were carefully selected under an optical microscope and glued to thin glass fibers. Structural measurements were performed on a computer-controlled Rigaku Mercury CCD Diffractometer with graphite-monochromated Mo Kα radiation ($\lambda_{MoK\alpha}$ = 0.71073 Å) at T = 293.2 K. Absorption corrections were made using the SADABS program.[11] The structures were solved using the direct method and refined by full-matrix least-squares methods on F^2 by using the SHELX-97 program package.[12] All non-hydrogen atoms were refined anistropically, and hydrogen atoms attached to carbon atoms were fixed at their ideal positions. And the water hydrogen atoms were located from difference maps and refined with isotropic temperature factors. Crystal data, as well as details of data collection and refinement of **1** and **2**, are summarized in Table 1. Selected bond lengths and angles are given in Table S1 (Supporting Information).

Computational Descriptions. The crystallographic data of complex **1** determined by X-ray were used to calculate the electronic band structure. Calculation of the electronic band structure along with density of states (DOS) was carried out with density functional theory (DFT) using one of the three nonlocal gradient-corrected exchange-correlation functionals (GGA-PBE) and performed with the CASTEP code,[13,14] which uses a plane wave basis set for the valence electrons and norm-conserving pseudopotential for the core electrons. The number of plane waves included in the basis was determined by a cutoff energy E_c of 450 ev. Pseudoatomic calculations were performed for C $2s^2 2p^2$, H $1s^1$, O $2s^2 2p^4$, and Zn $3d^{10} 4s^2$. The parameters used in the calculations and convergence criteria were set by the default values of the CASTEP code.[13]

Results and Discussion

Chiral PtS-Type Network in $[Zn(ip)]_n$ (1). An X-ray crystallographic analysis performed on compound **1** reveals an extended 3D coordination framework that crystallizes in the chiral space group $P4_32_12$ (no. 96), making it a chiral

(11) Sheldrick, G. M. *SADABS, Program for Area Detector Adsorption Correction*; Institute for Inorganic Chemistry, University of Göttingen: Göttingen, Germany, 1996.
(12) Sheldrick, G. M. *SHELXL-97, Program for Solution of Crystal Structures*; University of Göttingen: Göttingen, Germany, 1997.
(13) Segall, M.; Linda, P.; Probert, M.; Pickard, C.; Hasnip, P.; Clark, S.; Payne, M. *Materials Studio CASTEP*, version 2.2; Accelrys, Inc.: San Diego, CA, 2002.
(14) Segall, M.; Linda, P.; Probert, M.; Pickard, C.; Hasnip, P.; Clark, S.; Payne, M. *J. Phys.: Condens. Matter* **2002**, *14*, 2717.

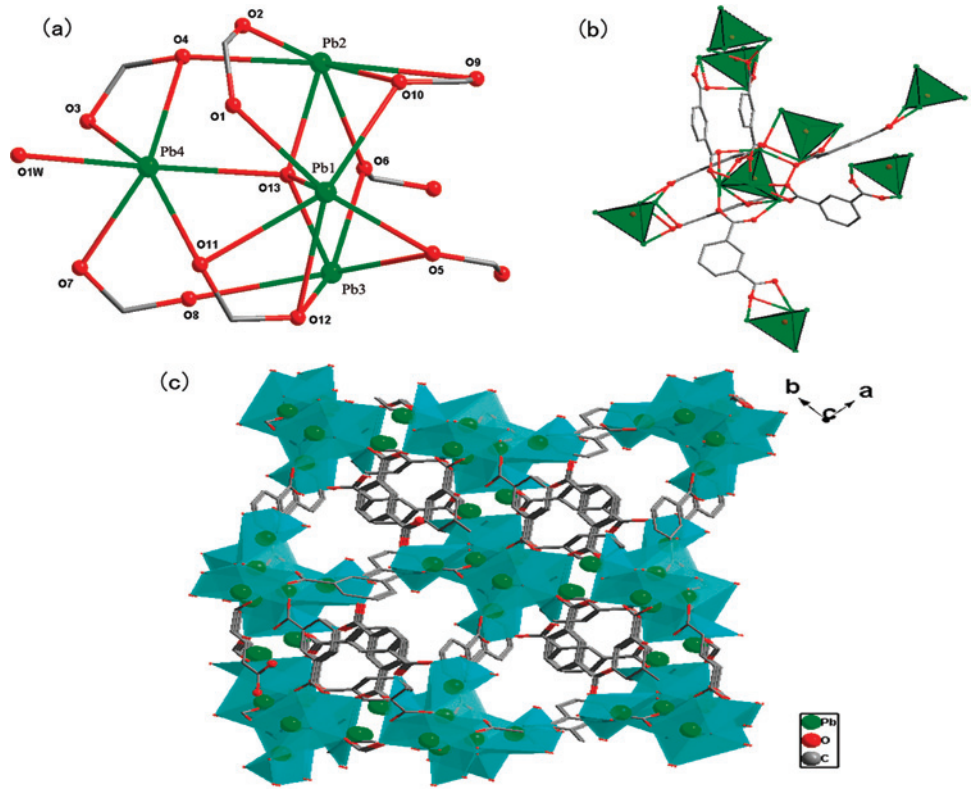

Figure 2. (a) Coordination environments of Pb(II) atoms in the tetrahedral Pb_4O cluster of complex **2**. (b) Perspective view of each Pb_4O cluster being connected to seven neighboring ones. (c) View of the 3D framework of **2**.

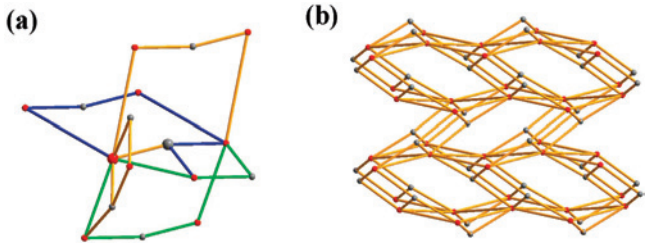

Figure 3. (a) A view of the essential circuits of each vertex (blue and green are seven-membered rings). (b) Schematic representation of the (3,7)-connected net in **2**.

compound based on ip ligands. There are three kinds of crystallographically independent Zn^{2+} ions in **1**, each in a slightly distorted tetrahedral geometry. And the molar ratio of Zn1 to Zn2 to Zn3 atoms is 1:2:1 (Figure 1b). Figure 1a illustrates that each Zn atom is coordinated by four oxygen atoms from four separate ip ligands. As shown in Table 2, the ip ligand features a μ_4-O,O′,O″,O‴ coordination mode. The adjacent tetrahedral Zn sites are connected to each other by the syn−anti bridging carboxylate groups, forming a Zn−carboxylate layer with $Zn_4(COO)_4$ rings. Then, each Zn−carboxylate layer is further linked to two neighboring layers by the ip ligands, resulting in the final 3D framework (Figure 1c). By considering the Zn atoms and ip ligands as tetrahedral and square-planar nodes, respectively, the framework of **1** can be described as a four-connected PtS net with a short vertex symbol 4^28^4 (Figure 1d).[15] It should be pointed out that only several reported chiral frameworks represent PtS-type topology.[16]

3D Connectivity Based on Pb_4O Clusters in $[Pb_4(\mu_4\text{-}O)(ip)_3(H_2O)]_n$ (2). Complex **2** is a three-dimensional network consisting of μ_4-O^{2-} anion-bridged Pb_4O tetrahedral clusters. There are four crystallographically distinct Pb^{2+} ions, three ip ligands, one terminal water molecule, and one O^{2-} anion in the asymmetric unit. As shown in Figure 2a, Pb1 is coordinated to six oxygen atoms with a distorted pentagonal pyramid geometry: one μ_4-oxygen atom (O13), two oxygen atoms (O11 and O12) from the same bridging carboxylate group of one ip ligand, and the other three oxygen atoms (O1, O5, and O10) from three carboxylate groups of three different ip ligands. The coordination environment of Pb2 is similar to Pb1. Pb3 adopts another kind of coordination manner. It coordinates with five oxygen atoms forming a distorted square-pyramid geometry: one μ_4-oxygen atom (O13) and the other four oxygen atoms (O5, O6, O8, and O12) from four carboxylate groups of four different ip ligands. Pb4 is surrounded by six oxygen atoms with a quite distorted pentagonal pyramid geometry: one μ_4-oxygen atom (O13), one (O1W) from the terminal water, two (O3 and O4) from the same bridging carboxylate group of an ip ligand, and the last two (O7 and O11) from two carboxylate groups of two different ip ligands. The μ_4-oxygen atom (O13) connects the four Pb(II) ions into a tetrahedral cluster. To our knowledge, such isolated tetrahedral Pb_4O clusters remain

(15) (a) Blatov, V. A.; Shevchenko, A. P.; Serezhkin, V. N. *Acta Crystallogr., Sect. A* **1995**, *51*, 909. (b) Blatov, V. A.; Carlucci, L.; Ciani, G.; Proserpio, D. M. *CrystEngComm* **2004**, *6*, 377.

(16) Zhang, J.; Bu, X. H. *Chem. Commun.* **2008**, 1756.

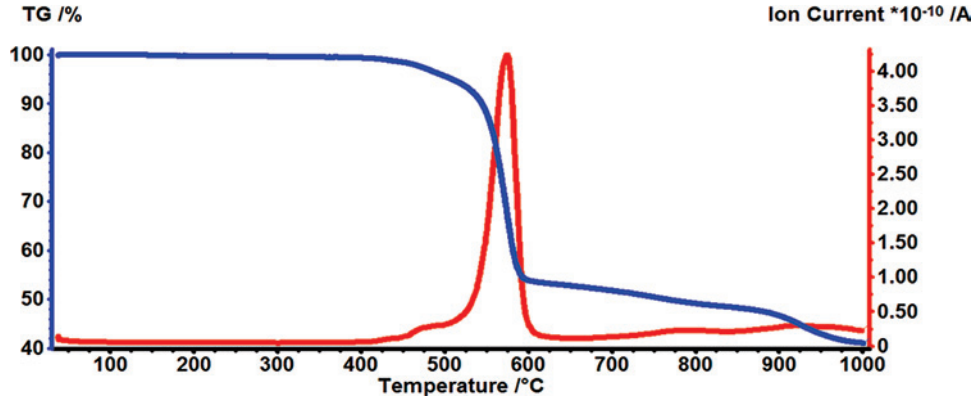

Figure 4. TGA coupled with QMS analyses of **1** with ion current signal for $m/z = 44$.

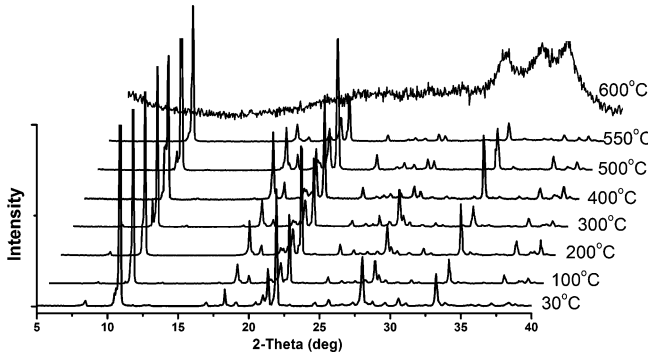

Figure 5. Variable-temperature PXRD patterns of **1** between 30 and 600 °C.

rarely reported.[17] Each tetrahedral cluster is linked to seven neighboring ones by seven ip ligands (Figure 2b). And according to the coordination modes, the seven ip ligands can be divided into three kinds (two μ_4-(η_2-O,O′),O,O″,O‴ ip ligands, two μ_5-(η_2-O,O′),(η_2-O″,O‴),O,O″,O‴ ip ligands, and three μ_6-O,O,O′,O′,O″,O‴ ip ligands). Although lots of ip complexes have been reported, the μ_6-O,O,O′,O′,O″,O‴ coordination mode has never been reported before. The μ_4-(η_2-O,O′),O,O″,O‴ ip ligand bridges two Pb_4O clusters. So does the μ_5-(η_2-O,O′),(η_2-O″,O‴),O,O″,O‴ ip ligand. However the μ_6-O,O,O′,O′,O″,O‴ ip ligand joins together three Pb_4O clusters. These ip ligands combine the Pb_4O clusters into the final 3D porous framework (Figure 2c).

Reticular chemistry is the basis for intricate MOF materials with interesting and useful properties, the core of which is to get better insight into the nature of nets using a knowledge of topology analysis and crystal chemistry. According to the above description, each μ_6-O,O,O′,O′,O″,O‴ ip ligand links three Pb_4O clusters, and each Pb_4O cluster links three μ_6-O,O,O′,O′,O″,O‴ ip ligands and four other Pb_4O clusters through two-connected μ_4-(η_2-O,O′),O,O″,O‴ ip ligands and μ_5-(η_2-O,O′),(η_2-O″,O‴),O,O″,O‴ ip ligands. So, we can define μ_6-O,O,O′,O′,O″,O‴ ip ligands and Pb_4O clusters as three-connected and seven-connected nodes, respectively. In this case, the net in **2** represents a novel (3,7)-connected topology (Figure 3b). Those rings which represent the smallest circuit of the essential rings that define the topology of **2** are shown in Figure 3a. The long Schläfli symbol for three-connected nodes is 3.4.5, and for seven-connected nodes is $3.3.4.4.4.4.4.5.5.5.5.5.6.6.6.6.6.6_2.6_2.7.7_3$. So the short symbol for this (3,7)-connected net becomes (3.4.5)-($3^2.4^5.5^6.6^7.7^2$). It is worth noting that this (3.4.5)-($3^2.4^5.5^6.6^7.7^2$) net is first reported here, and even a MOF with a (3,7)-connected net has never come forth.

In summary, we have obtained two 3D MOF materials by the assembly of isophthalic acid and Zn^{2+} or Pb^{2+} ions under similar conditions. They represent different topologies, which might be due to the different coordination behaviors of Zn^{2+} and Pb^{2+} ions. Complex **1** has a chiral PtS-type network, which is constructed by ip ligands connecting isolated four-coordinated Zn atoms. Whereas, **2** contains a first-reported (3,7)-connected (3.4.5)($3^2.4^5.5^6.6^7.7^2$) net, which is obtained on the basis of the tetrahedral Pb_4O cluster secondary building units.

Thermogravimetric Analysis (TGA-MS) and XRD Patterns. To study the thermal stability of the two complexes, TGA coupled with QMS analysis was performed on polycrystalline samples under a N_2 atmosphere with a heating rate of 10 °C min^{-1} in the temperature range 30−1000 °C. Complex **1** remains stable up to ~500 °C, and mass fragment 44 m/z corresponding to CO_2 is also observed in the range 500−600 °C (Figure 4). This indicates that **1** represents high stability compared with the easy decomposability of other reported NLO MOF materials, extending its potential applications. Variable-temperature powder X-ray diffraction (PXRD) further confirms that the framework of **1** can even be retained until 550 °C is reached (Figure 5).

TGA-MS data show the thermal ability of **2** to ~300 °C (Figure 6). A small part of the samples decomposes in the range 300−400 °C, coupled with a low ion current signal of CO_2 ($m/z = 44$). Then, the whole framework quickly collapses above 400 °C, and a distinct mass fragment of CO_2 appears in the 400−700 °C range. PXRD patterns also confirm its thermal stability (Figure S4, Supporting Information).

Optical Properties. As shown in Figures S1 and S2 in the Supporting Information, IR spectral shapes of the two complexes are slightly different. For complex **1**, the characteristic bands at 1601−1538 cm^{-1} and 1467−1408 cm^{-1} should be assigned to the asymmetric vibration and sym-

(17) (a) Gaffney, C.; Harrison, P. G.; King, T. *Chem. Commun.* **1980**, 1251. (b) Zhang, Z.; Zhou, Y. L.; He, H. Y. *Acta Crystallogr., Sect. E* **2006**, *62*, m2591.

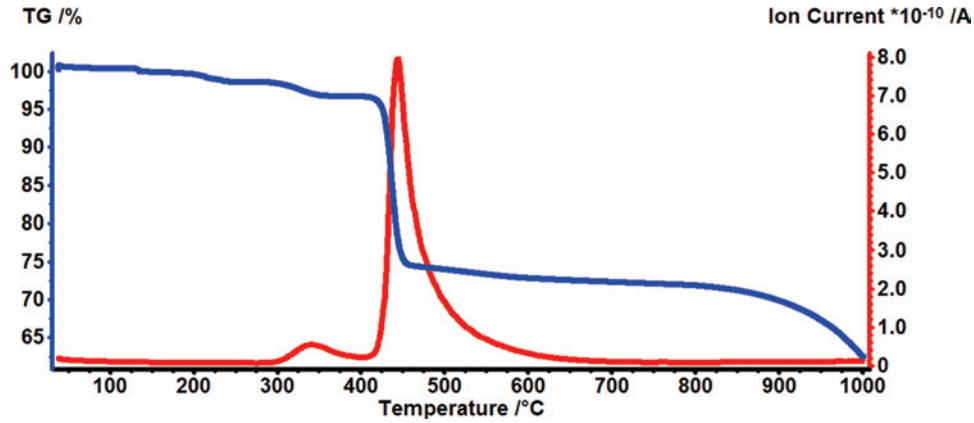

Figure 6. TGA coupled with QMS analyses of **2** with ion current signal for $m/z = 44$.

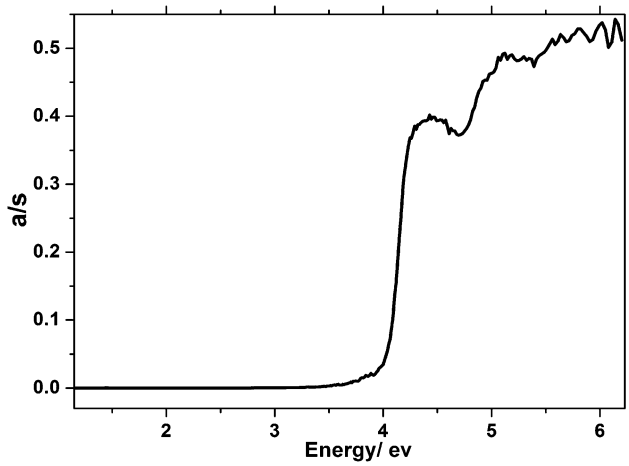

Figure 7. Optical diffuse reflectance spectra for **1**.

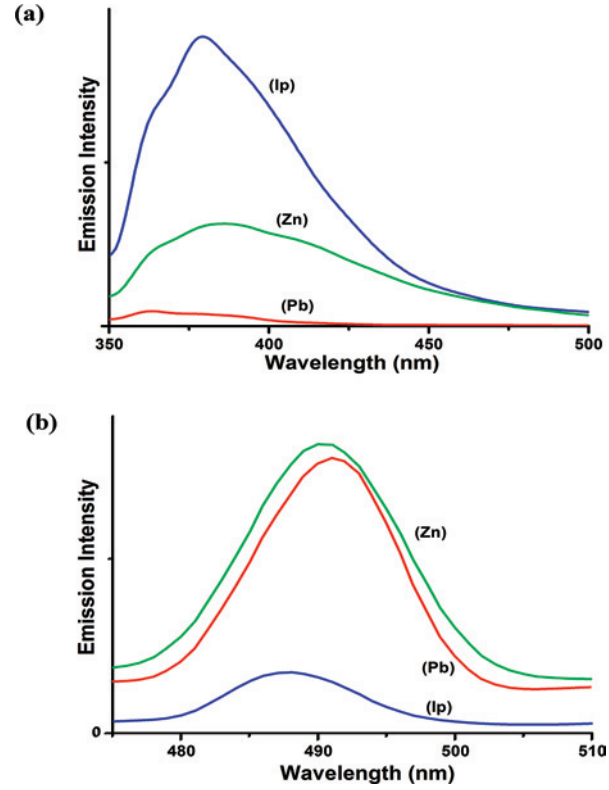

Figure 8. Emission spectra for **1**, **2**, and isophthalate acid in the solid state at room temperature in the UV area (a) and visible area (b), showing the different intensities (green for **1**, red for **2**, blue for isophthalate acid).

metric vibration of the carboxylate groups, respectively. For complex **2**, the peaks of asymmetric vibration and symmetric vibration of the carboxylate groups are at 1602−1518 cm^{-1} and 1432−1362 cm^{-1}, respectively. The $\Delta\nu$ (ν_{as}(COO) − ν_s(COO)) value is about 130 cm^{-1} for **1** and 160 cm^{-1} for **2**, suggesting that the carboxylate groups in the two complexes coordinate to the metal centers in the bridging mode. And the absence of the characteristic band at ca. 1700 cm^{-1} attributed to the protonated carboxylate groups indicates that all carboxylate groups in **1** and **2** are deprotonated,[18] which is consistent with the X-ray structural analytical results.

The UV absorption spectrum of complex **1** indicates that it is transparent in the range of 400−1100 nm (Figure S3, Supporting Information). From 400 to 200 nm, the absorption increases quickly with the decreasing wavelength. An optical diffuse reflectance study of **1** reveals an optical band gap of 3.9 eV, making it a wide band gap semiconductor (Figure 7).

The luminescent properties of the two complexes in the solid state at room temperature have also been studied. As shown in Figure 8, both of the compounds show two emission bands. They are at 393 nm (λ_{ex} = 320 nm) and 493 nm (λ_{ex} = 208 nm) for **1** and 362 nm (λ_{ex} = 330 nm) and 493 nm (λ_{ex} = 208 nm) for **2**. In order to understand the nature of these emission bands, we also measured the luminescent properties of free isophthalate acid. It also has two similar emission bands, 378 nm (λ_{ex} = 338 nm) and 488 nm (λ_{ex} = 238 nm). So the emission bands of **1** and **2** might be attributed to the intraligand emission from ip ligands. Of note is that there are observable differences between the intensity of the emission bands of the free ligand and the two complexes under the same experimental conditions. The UV emission intensity of free ip is much stronger than that of the two complexes. However, the order in the visible region is just reversed. And there are also changes between the emission bands of **1** and **2**. These differences might be due to the fact that the photoluminescence behavior

(18) Nakamoto, K. *Infrared and Raman Spectra of Inorganic and Coordination Compounds*, 4th ed.; John Wiley & Sons: New York, 1986.

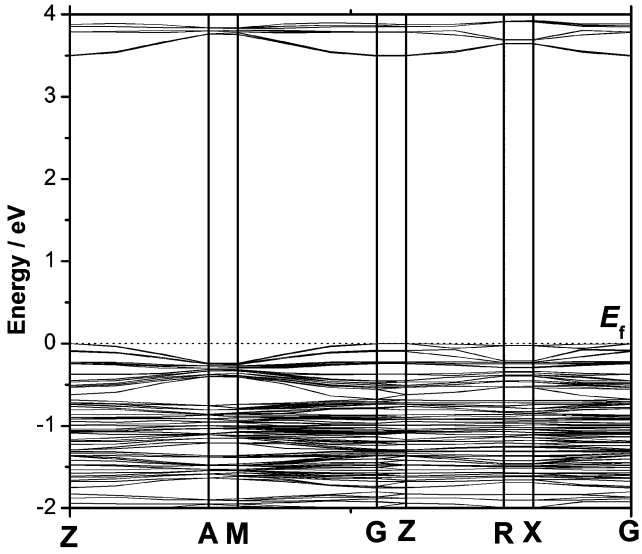

Figure 9. Calculated energy band structure of **1**.

Table 3. The State Energies (eV) of the Lowest Conduction Band (L-CB) and the Highest Valence Band (H-VB) at Some *k* Points for Crystal **1**

k point	Z	A	M	G	R	X
L-CB	3.49601	3.76478	3.75702	3.49409	3.64281	3.64295
H-VB	0	−0.24155	−0.23758	−0.00044	−0.02531	−0.025

is closely associated with the metal ions and the coordination status of the ligands.[19]

Second Harmonic Generation (SHG) Measurements. Complex **1** is acentric with a space group $P4_32_12$. Hence, its second-order NLO properties are worth studying. The intensity of the green light (frequency-doubled output: $\lambda =$ 532 nm) produced by the powder sample of compound **1** is about 1.5 times that produced by a potassium dihydrogen phosphate (KDP) powder, indicating that compound **1** has a SHG effect that is stronger than that of KDP.[20] Although lots of noncentrosymmetric or enantiomorphic isophthalic acid MOFs have been reported, the NLO properties of them have never been researched.[21] And according to the above discussion, **1** exhibits remarkable thermal stability and is transparent in the range of 400−1100 nm and insoluble in common solvents, making it a potential candidate for practical applications.

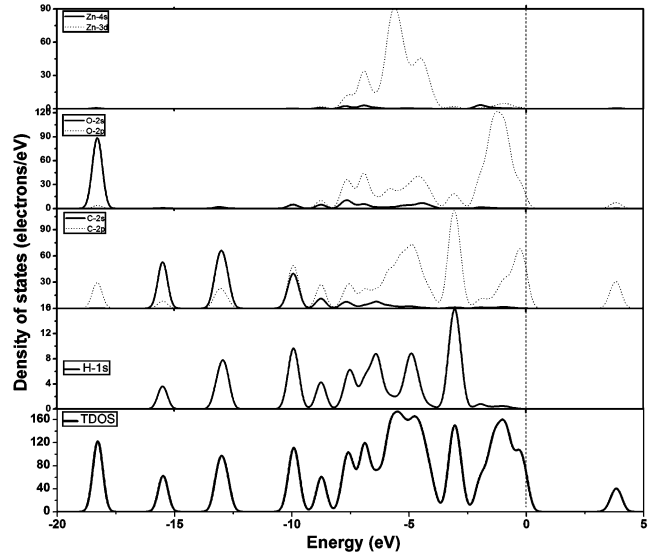

Figure 10. The TDOS and PDOS of **1**.

Theoretical Studies. In order to understand the relation between the structure and physical properties better, we have researched the band structure and densities of states of compound **1** using the DFT method, which has rarely been carried out on metal−organic complexes. The calculated band structure of complex **1** along high symmetry points of the first Brillouin zone is plotted in Figure 9. It is found that both the top of valence bands (VBs) and the bottom of conduction bands (CBs) display a small dispersion. The state energies (eV) of the lowest conduction band (L-CB) and the highest valence band (H-VB) at some *k* points of compound **1** are listed in Table 3. The lowest of the CBs is localized at the G point and has an energy of 3.4941 eV. And the energy of the VBs at the G point is −0.0004 eV. Accordingly, it is reasonable to consider **1** as a wide band gap semiconductor with a band gap of around 3.49 eV. The calculated band gap of **1** is slightly smaller than the experimental one (3.9 eV). The discrepancy is due to the limitation of the DFT method that sometimes underestimates the band gap in semiconductors and insulators.[22]

The bands can be assigned according to the total and partial densities of states (TDOS and PDOS, respectively) as shown in Figure 10. The bands just above the Fermi level (the Fermi level is set at the top of the valence band) are derived from C-2p with small mixing of the O-2p state in the range 2.78−4.83 eV. The bands below the Fermi level can be divided into five regions. The VBs around −18.27 eV are composed of the states O-2s and C-2p. The H-1s, C-2s, and C-2p states give rise to the VBs lying near −15.49, −12.99, −9.92, and −8.74 eV. The VBs ranging from −8.23 to −3.66 eV result from the states of H-1s, C-2p, O-2p, and Zn-3d. The VBs around −3.06 eV are dominated by H-1s and C-2p states. And the VBs from −2.41 to 0.88 eV are mostly formed by the O-2p states with the mixings of C-2p and H-1s states.

(19) (a) Dai, J. C.; Wu, X. T.; Fu, Z. Y.; Cui, C. P.; Wu, S. M.; Du, W. X.; Wu, L. M.; Zhang, H. H.; Sun, Q. *Inorg. Chem.* **2002**, *41*, 1391. (b) Wang, X. L.; Qin, C.; Li, Y. G.; Hao, N.; Hu, C. W.; Xu, L. *Inorg. Chem.* **2004**, *43*, 1850.

(20) The powder second-harmonic generation test was carried out on the sample by the Kurtz and Perry method. Second-harmonic generation intensity data were obtained by placing a sieved (80−100 mesh) powder sample in an intense fundamental beam from a Q-switched Nd:YAG laser of wavelength 1064 nm. The output ($\lambda = 532$ nm) was filtered first to remove the multiplier and was then displayed on an oscilloscope. This procedure was then repeated using standard NLO material (microcrystalline KDP), and the ratio of the second-harmonic intensity outputs was calculated.

(21) (a) Otto, T. J.; Wheeler, K. A. *Acta Crystallogr., Sect. C* **2001**, *57*, 704. (b) Wan, Y.; Zhang, L.; Jin, L.; Gao, S.; Lu, S. *Inorg. Chem.* **2003**, *42*, 4985. (c) Wan, Y.; Zhang, L.; Jin, L. *J. Mol. Struct.* **2003**, *658*, 253. (d) Abourahma, H.; McManus, G. J.; Moulton, B.; Walsh, R. B.; Zaworotko, M. J. *Macromol. Symp.* **2003**, *196*, 213. (e) He, J.; Zhang, J. X.; Tan, G. P.; Yin, Y. G.; Zhang, D.; Hu, M. H. *Cryst. Growth Des.* **2007**, *7*, 1508. (f) Dai, Y. M.; Ma, E.; Tang, E.; Zhang, J.; Li, Z. J.; Huang, X. D.; Yao, Y. G. *Cryst. Growth Des.* **2005**, *5*, 1313.

(22) (a) Godby, R. W.; Schluther, M.; Sham, L. *J. Phys. Rev. B* **1987**, *36*, 6497. (b) Okoye, C. M. I. *J. Phys.: Condens. Matter* **2003**, *15*, 5945.

Conclusions

In this paper, two new 3D MOF materials bridged by isophthalate ligands, $[Zn(ip)]_n$ (**1**) and $[Pb_4(\mu_4\text{-}O)(ip)_3(H_2O)]_n$ (**2**), have been prepared and characterized. Both compounds are photoluminescent and feature interesting topology nets, with a PtS-type net for **1** and a first-reported (3,7)-connected net for **2**. Moreover, **1** displays a moderately strong SHG signal of an intensity about 1.5 times that of KDP. It is stable up to ∼500 °C and transparent in the range 400−1100 nm, making it a potential NLO material in the visible region. And both the experimental spectrum and the calculated band structure show that **1** possesses semiconducting features with a wide band gap. We have also assigned the bands to the total and partial densities of states. Herein, such theoretical research based on DFT methods has been unwontedly actualized in the area of MOFs. This may help us understand the structures of MOFs in depth, which may be propitious to exploring new NLO MOF materials.

Acknowledgment. This work was supported by the State Key Basic Research and Development Plan of China (2007CB815302), the Chinese Academy of Sciences (KJCX2-YW-M05), the NSF (E0620005) of Fujian Province, the Major Special Foundation of Fujian Province (2005HZ1027 and 2005HZ01-1), the Fund of Fujian Key Laboratory of Nanomaterials (2006L2005), and the Knowledge Innovation Program of the Chinese Academy of Sciences.

Supporting Information Available: Crystallographic data in CIF format for compounds **1** and **2**, X-ray powder diffraction patterns for compound **2**, selected bond lengths and angles for compounds **1** and **2**, IR spectrums for **1** and **2**, and an UV absorption spectrum for **1**. These materials are available free of charge via the Internet at http://pubs.acs.org.

IC800871R